Thermal Lensing in a Nd:YAG Laser Rod

W. Koechner

Theoretical and experimental results are reported on the thermal lensing effect caused by the radial thermal gradient present in optically pumped Nd:YAG laser rods. The presented theory is in agreement with the experimental observations. The results reveal that a Nd:YAG rod under pumped light becomes a positive lens with two focal lengths. The temperature dependent variation of the refractive index constitutes the major contribution of the thermal lensing. The stress dependent variation of the refractive index modifies the focal length about 20%. The effect of end-face curvature caused by an elongation of the rod is less than 6%.

I. Introduction

Any solid laser material operating in either the steady state or cw mode of operation must dissipate an appreciable amount of heat. The heat arises from the radiationless transitions in the material, i.e., the energy differential from pump to fluorescent bands, and a quantum efficiency less than one. In the cylindrical geometries generally used, the heat is removed on the circumferential surface of the cylinder, thereby generating a radial thermal gradient. The change in temperature within a laser rod causes a thermal distortion of the laser beam due to a temperature and stress dependent variation of the refractive index. In addition, the generated stresses induce birefringence. The knowledge of the heat dissipated by the YAG rod permits one to calculate the radial temperature gradient, and, subsequently, stresses and strain, change of index of refraction, thermal lensing, and birefringence in the crystal can be computed.

Thermal lensing has been discussed by Osterink.[1] In this paper, a detailed analysis is presented of the various effects contributing to thermal lensing. The presented theory is in good agreement with the experimental observations.

The experiments were performed with a cw pumped Nd:YAG crystal 7.6 cm long and 6.39 mm in diameter. The crystal was pumped by two water cooled cw arc lamps filled with krypton. The pumping cavity consisted of a double elliptical cylinder. Cooling of the rod was accomplished by circulating water in a jacket surrounding the crystal. The cw output power of this laser was 250 W at an input of 12 kW.

II. Theory

For a cylindrical rod with thermal conductivity K, in which heat is uniformly generated at a rate A_0 per unit volume, the steady state temperature at any point along a radius of length r is given by[2]

$$T(r) = T_0 - A_0 r^2 / 4K, \qquad (1)$$

where T_0 is the temperature at the center of the rod. A_0 is given by

$$A_0 = P_a / \pi r_0^2 L, \qquad (2)$$

where P_a is the dissipated power in the crystal, r_0 is the radius, and L is the length of the rod, respectively.

If η is the fraction of the electrical input power P_{in} into the lamps which is dissipated as heat in the rod, then

$$P_a = \eta P_{in}. \qquad (3)$$

This equation assumes that the heat generated in the rod is directly proportional to the power input to the lamps. Upon substitution of A_0, one obtains from Eq. (1)

$$T(r) = T_0 - \eta P_{in} r^2 / 4K \pi L r_0^2. \qquad (4)$$

The thermal radial gradient as given by Eq. (4) introduces a radial variation of the refractive index. The change of the refractive index can be separated into a temperature and a stress dependent variation. Hence

$$n(r) = n_0 + \Delta n(r)_T + \Delta n(r)_\epsilon, \qquad (5)$$

where $n(r)$ is the radial variation of the refractive index, n_0 is the refractive index at the center of the rod, $\Delta n(r)_T$ and $\Delta n(r)_\epsilon$ are the temperature and stress dependent changes of the refractive index, respectively.

The temperature dependent change of refractive

The author is with the Korad Department, Union Carbide Corporation, Santa Monica, Calif. 90406.

index can be expressed as

$$n(r)' = n_0 + (\delta n/\delta T)[T(r) - T_0]. \tag{6}$$

Substitution of Eq. (4) into Eq. (6) gives

$$n(r)' = n_0 - (P_{in}r^2\eta/4K\pi Lr_0^2)(\delta n/\delta T), \tag{7}$$

or

$$\Delta n(r)_T = c_1(r^2/r_0^2), \tag{8}$$

where

$$c_1 = -(\eta P_{in}/4K\pi L)(\delta n/\delta T). \tag{9}$$

The refractive index of a crystal is specified by the indicatrix, which is an ellipsoid whose coefficients are the components of the relative dielectric impermeability tensor.

A change of refractive index produced by stress is given by a small change in shape, size, and orientation of the indicatrix.[3] The change is specified by the small changes in the coefficients B_{ij}. Neglecting the electro-optic effect, the changes ΔB_{ij} are given by[4]

$$\Delta B_{ij} = p_{ijkl}\epsilon_{kl}(i,j,k,l = 1,2,3), \tag{10}$$

where p_{ijkl} is a fourth rank tensor giving the photo-elastic effect. The elements of this tensor are the elas-tooptical coefficients. ϵ_{kl} is a second rank strain tensor.

Since YAG is a cubic crystal, the indicatrix is a sphere. Under stress the indicatrix becomes an ellipsoid. Nd:YAG rods are grown with the cylindrical axes along the [111] direction. The light propagates in this direction and thus the change of the refractive index along the [111] direction is of interest. The equation of the indicatrix, for a plane perpendicular to the [111] direction, is given:

$$(B^\circ + \Delta B_{x^*x^*})x^{*2} + (B^\circ + \Delta B_{y^*y^*})y^{*2} = 1. \tag{11}$$

This equation was obtained by transforming to the principal coordinate system of the ellipse, where the orientation of the x^* and y^* are shown in Fig. 1.

The effect of $\Delta B_{x^*x^*}$ and $\Delta B_{y^*y^*}$ is to change the refractive index for a wave polarized along x^* and y^*, respectively. With

$$B^\circ = (n_0^2)^{-1} \tag{12}$$

and

$$\Delta n_{x^*} = -\tfrac{1}{2}(n_0^3)\Delta B_{x^*x^*}, \qquad \Delta n_{y^*} = -\tfrac{1}{2}(n_0^3)\Delta B_{y^*y^*}, \tag{13}$$

and upon substitution of $\Delta B_{x^*x^*}$ and $\Delta B_{y^*y^*}$ by the expression derived in the Appendix, one obtains

$$\Delta n(r)_{\epsilon x^*} = c_2 + c_3(r^2/r_0^2), \tag{14}$$

$$\Delta n(r)_{\epsilon y^*} = c_4 + c_5(r^2/r_0^2), \tag{15}$$

where the parameters c_2, c_3, c_4, and c_5 are defined in Eqs. (A15) to (A17).

As can be seen from these expressions, the refractive index is a parabolic function with radius. The change of refractive index due to thermal strain is dependent on the polarization of the light. The radial component of the wave experiences a change given by $\Delta n(r)_{\epsilon x^*}$ whereas the tangential component changes as given

by $\Delta n(r)_{\epsilon y^*}$. This means that a wave incident on the crystal is focussed at two different focal points.

Introducing Eqs. (14), (15), and (8) into (5) gives the total radial variation of the refractive index.

$$n(r)_{\epsilon x^*} = n_0 + c_2 + (c_1 + c_3)(r^2/r_0^2), \tag{16}$$

$$n(r)_{\epsilon y^*} = n_0 + c_3 + (c_1 + c_5)(r^2/r_0^2). \tag{17}$$

The focal length of the YAG rod can be derived from these equations by applying formulas given by Kogelnik[5] for a lenslike medium. The focal length of a section of length L for a lenslike medium is, according to Kogelnik,

$$f = b(2n'_0 \sin 2L/b)^{-1}. \tag{18}$$

Where the refractive index is assumed to vary near the optic axis, as in

$$n = n'_0(1 - 2r^2/b^2), \tag{19}$$

the distance h of the principal planes from the ends of the lenslike medium is given by

$$h = b/2n'_0 \tan(L/b). \tag{20}$$

Comparing Eqs. (19) and (16) gives

$$n'_0 = n_0 + c_2, \tag{21}$$

and

$$b^2 = -2(n_0 + c_2)r_0^2/(c_1 + c_3). \tag{22}$$

The focal length of the Nd:YAG rod under thermal stress is then obtained from Eq. (18).

The numerical values reveal that $2L \ll b$ and $c_2 \ll n_0$. Therefore,

$$\sin (2L/b) \approx 2L/b \text{ and } n'_0 \approx n_0.$$

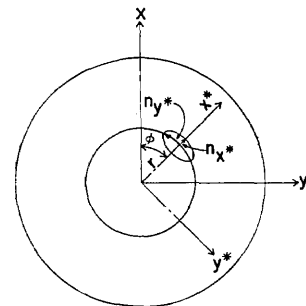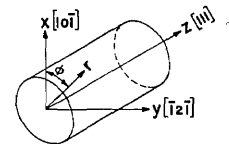With these approximations, the focal length of the rod is

Fig. 1. Crystal orientation for a YAG rod (top) and orientation of indicatrix of a thermally stressed YAG rod in a plane perpendicular to the rod axis (bottom).

$$f' = b^2/4n_0L. \qquad (23)$$

The distance h of the principal planes from the ends becomes

$$h = L/2n_0. \qquad (24)$$

Before a final expression for the focal length is obtained, the contributions caused by end effects will be calculated.

Perturbations on the principal thermal distortion pattern occurs in laser rods near the ends where the free surface alters the stress character. The so-called end effects account for the physical distortion in the flatness of the rod ends. End effects in glass rods have been considered by Snitzer[6] and La Marre.[7] Self equilibrating stresses causing a distortion of flatness was found to occur within a region of approximately one diameter from the ends. The thermal gradient in sections of the rod further away from the ends does not contribute to the elongation of the rod. Instead, the crystal is under compression and stresses are generated. The elongation of the rod can be expressed as

$$l(r) = l_0 + (\delta l/\delta T)(T(r) - T_0), \qquad (25)$$

where l_0 is the length of the end section of the rod over which expansion occurs, and

$$\delta l/\delta T = \alpha l_0, \qquad (26)$$

where α is the thermal expansion coefficient.

Measurements performed on YAG rods (see Fig. 6) indicate that the distortion of the flatness of the rod can be best described by assuming an end section over which expansion occurs to be approximately equal to the radius of the rod ($l_0 \approx r_0$). The radius of the end face curvature at each end of the rod follows from Eq. (25):

$$R = -(d^2l/dr^2)^{-1}. \qquad (27)$$

Introducing the parameters given by Eqs. (25) and (4) into Eq. (27) yields

$$R = 2K\pi Lr_0^2/\alpha\eta P_{in}l_0. \qquad (28)$$

The focal length of the rod caused by an end face curvature is obtained from the thick lens formula of geometric optics.[4] It is

$$f'' = R/2(n_0 - 1). \qquad (29)$$

The final expression for the total focal length of the rod is obtained by combining Eqs. (23) and (29):

$$f = \left(\frac{1}{f'} + \frac{1}{f''}\right)^{-1} = \left[\frac{4n_0L}{b^2} + \frac{2(n_0 - 1)}{R}\right]^{-1}. \qquad (30)$$

Upon substitution of b by Eq. (22), and R by Eq. (28) gives

$$f_1 = \frac{2K\pi r_0^2}{P_{in}\eta}\left[\frac{\delta n}{\delta T} - \frac{n_0^3\alpha c''_x}{48(1 - \nu)} + \frac{2(n_0 - 1)\alpha l_0}{L}\right]^{-1}. \qquad (31)$$

The first term in the bracket of Eq. (31) represents the contribution of the temperature dependent change of the refractive index. The second term represents the stress dependent change of the refractive index. The last term gives the distortion caused by the end face curvature of the rod. Equation (31) gives the focal length f_1 of all rays polarized in radial direction. Substitution of c''_x by c''_y results in another focal length f_2 for rays polarized in tangential direction. Since a linear polarized wave or a nonpolarized wave incident on the crystal will have components in radial and tangential direction, two focal points are obtained.

Introducing materials and operational parameters into the equations results in an expression relating the focal length of the rod to the electrical lamp input power.

For Nd:YAG, the approximate values of the elasto-optical coefficients are[8] $p_{11} = -0.0290$, $p_{12} = +0.0091$, and $p_{44} = -0.0615$.

Also for Nd:YAG, the following constants are given[9]: ν is the 0.3 Poisson ratio; n_0 is the 1.823 refractive index; α, the $7.9 \times 10^{-6}/°C$ thermal expansion coefficient; K is 0.111 W/cm°C thermal conductivity of YAG at 70°C; and $dn/(dt)$, the $7.3 \times 10^{-6}/°C$ change of refractive index with temperature.[10] The length of the crystal was $L = 7.5$ cm, and the radius $r_0 = 0.31$ cm.

The fraction of heat dissipated by the crystal to electrical lamp input was measured[11] $\eta = 5 \times 10^{-2}$. This number was obtained from a calorimetric measurement of the heat extracted in the rod cooling loop with and without the Nd:YAG crystal in the pumping cavity. With these numerical values and the parameters $c''_x = -1.311$ and $c''_y = 0.17$ from Eqs. (A10) and (A11), one obtains for the two focal lengths of the YAG crystal

$$f_1 = 1.41/P_{in}, \qquad (32)$$

$$f_2 = 2.0/P_{in}, \qquad (33)$$

where f_1 and f_2 are in meters and P_{in} is in kilowatts. Both functions are plotted in Fig. 3. Comparing the three terms in the bracket of Eq. (31) reveals that

$$\frac{\delta n}{\delta T} > \frac{n_0^3\alpha c''_x}{48(1 - \nu)} > \frac{2(n_0 - 1)\alpha l_0}{L}.$$

In the expression for f_1, for example, the ratio of these terms is 7.3:1.88:0.54. This means that the temperature dependent variation of the refractive index represents the largest contribution to thermal lensing.

III. Experiments

Figure 2 shows the experimental setup for the measurement of the effective focal length with a He–Ne gas laser. The collimated output from the gas laser operated at 6328 Å is passed through the YAG crystal, the beam waist is measured as a function of the distance from the second principal plane of the rod. The distance of the principal planes from the ends of the rod is $h = 2.05$ cm.

For each given lamp input power two focal points were observed as predicted by the theory. However, the presence of two focal points made it difficult to determine exactly each focal length. In addition, the measurements were complicated by the large amount of stray pump light incident on the screen, and by the
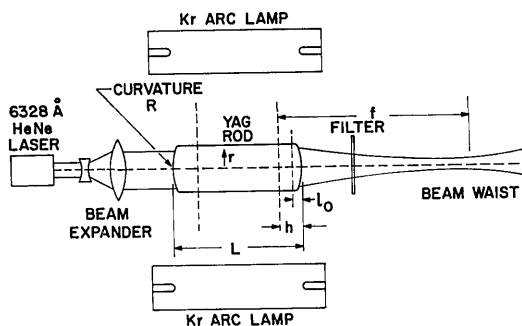
Fig. 2. Experimental setup for the measurement of the effective focal length with a gas laser.

fact that for high input powers the focal points were inside the structure of the laser head. The result of the measurement is shown in Fig. 3. The values plotted in this figure represent the average focal length of the rod as a function of the lamp input power. As can be seen, the experimental data agrees fairly well with the theoretical values, especially in view of the fact that, due to the difficulties mentioned above, the accuracy of the measurements is probably not better than 20%.

As can be seen, the effective focal length is 10 cm at maximum input. This illustrates the large effect of the optical distortion. No difference in effective focal length has been found if the rod was pumped with the mirror removed or when the rod was actually lasing between flat mirrors.

The effective focal length of the rod was also calculated by operating the optical resonator at the limit of stable operation. From the theory of resonators by

Kogelnik[5] follows that a resonator is stable if $-1 \leq G_1 G_2 \leq +1$, where G_1 and G_2 are dimensionless parameters describing the design of the resonator. For a resonator with internal optical elements, these factors are given by Kogelnik as:

$$G_1 = \frac{a_1}{a_2}\left[1 - \frac{d_2}{f} - \frac{1}{R_1}\left(d_1 + d_2 - \frac{d_1 d_2}{f}\right)\right], \qquad (34)$$

$$G_2 = \frac{a_2}{a_1}\left[1 - \frac{d_1}{f} - \frac{1}{R_2}\left(d_1 + d_2 - \frac{d_1 d_2}{f}\right)\right], \qquad (35)$$

where a_1 and a_2 are the apertures of the mirrors 1 and 2, and d_1 and d_2 are the distances from the principal planes.

In our experiments flat mirrors with identical apertures have been used separated at equal distances from the YAG crystal.

Therefore,

$$a_1 = a_2, \ R_1 = R_2, \text{ and } d_1 = d_2 = d.$$

Equations (34) and (35) simplify, and we have

$$G_1 = G_2 = 1 - d/f. \qquad (36)$$

Figure 4 shows the stability diagram of an optical

Fig. 4. Stability diagram of an optical resonator. Shaded areas indicate regions of unstable operation. Points A, B, and C correspond to plane parallel, confocal, and concentric resonators, respectively.
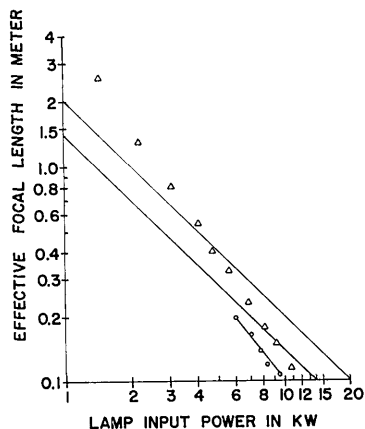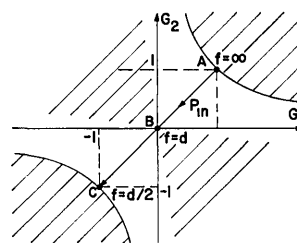

Fig. 3. Effective focal length of YAG crystal as a function of lamp input power. The two theoretical focal lengths according to Eq. (31) are plotted (solid lines) together with experimental values obtained with a gas laser ($\triangle$) and values obtained from resonator theory ($\bigcirc$).

resonator as given by Kogelnik.[12] The straight line gives the position of a symmetrical resonator with an internal lens of different focal length. Since the thermal lensing of the crystal is a function of input the equivalent resonator configuration changes from plane parallel, to confocal and finally to concentric. Beyond this point the resonator becomes unstable. In our experiments the mirror separation had been changed until the resonator became unstable, which is evident by a decrease of output power for increasing input powers. This was done for several input power levels. At the point of unstable operation (see Fig. 4) the effective focal length of the rod is given by:

$$f = d/2. \qquad (37)$$

The result of these measurements is also shown in Fig. 3. The interpretation of the point of unstable

operation is complicated by the fact that the laser output was multimode, whereas Eqs. (34)–(37) are strictly valid only for gaussian beams.

The values of the effective focal length as derived from the resonator theory are lower than the values obtained with the gas laser. However, the deviation is within the accuracy of these two methods which we believe is in the order of $\pm 20\%$.

In order to check the degree of physical distortion in the flatness of the rod ends under pump light an experiment as shown in Fig. 5 was performed. The collimated beam of a He–Ne gas laser reflected off the first surface of the Nd:YAG crystal was displayed on a screen. An increase in spot size of the reflected beam was observed, depending on the lamp input power. If d_0 and d_1 are the spot sizes of the reflected gas laser beam with and without pumping of the YAG crystal, then

$$R = \frac{2t}{d_1/d_0 - 1},\tag{38}$$

where R is the radius of the crystal front surface and $t = t_1 + t_2$ is the distance from the reflecting surface to the screen.

A noticeable change in spot size occurred only at relatively high input powers. With $t = 3$ m and $d_0 = 0.53$ cm, the maximum spot size observed was $d_1 = 1.06$ cm at 12 kW pump power in the lamps. The result of the measurements is shown in Fig. 6. The strongest curvature of the rod ends occurring at maximum lamp input power was measured to be $R = 6$ m.

Figure 6 also contains the theoretical values for the radius of the end face curvature as obtained from Eq. (28) for two values of $l_0 = r_0$ and $l_0 = r_0/2$. One obtains $R = 41/P_{in}$ and $R = 82/P_{in}$, respectively, where R is in meters and P_{in} in kilowatts.

IV. Compensation of Thermal Lensing

As discussed in the last chapter, a focusing rod between flat mirrors is equivalent to a passive resonator having curved mirrors. It is well known from resonator theory[15] that stronger curved mirrors result in smaller
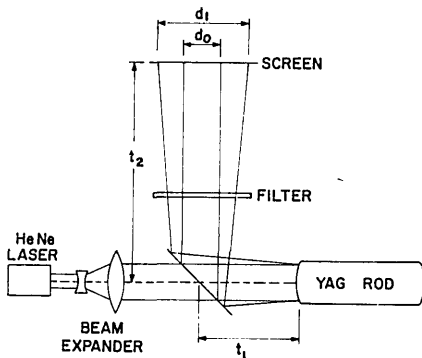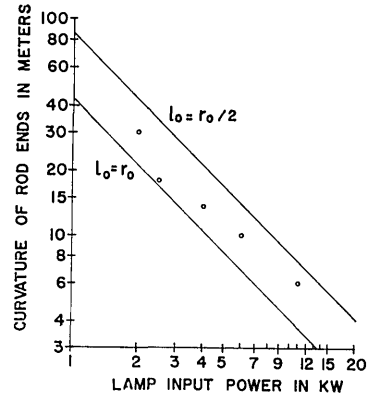

Fig. 6. Theoretical (solid lines) and experimental (O) values of the end face curvature of a YAG rod as a function of lamp input power.

diffraction losses for higher order modes. Thus the beam divergence of the laser increases according to $\Theta_{mn} = c_{mn}K$, where K is a constant and c_{mn} is the ratio of radii of different modes with respect to the lowest order mode. The value of c_{mn} increases for increasing mode numbers. In order to increase brightness of our laser, we compensated for the spherical component of the positive thermal lensing exhibited by the rod. This was done by grinding negative spherical surfaces on the ends of the rod. Although thermal lensing of the rod is a volume effect, it can be treated in a first order approximation, as if the focusing would be caused by a positive end face curvature.

Several rods were polished with negative curvatures on the ends. Since the rods were operated between flat mirrors, it is desirable to undercompensate the rod in order to achieve stable operation. For example, we tested a rod with a $R = -0.5$-m curvature on both ends. According to Eq. (29), this gives a negative focal length of $f = -0.3$ m. The rod would therefore be thermally compensated at an input level of 6 kW. Operation of the crystal in the laser head revealed that the threshold of this rod went up a factor of two. The output was very unstable at low output powers. However, above the compensation point as measured with a He–Ne laser, the output power was very stable and the beam divergence decreased by a factor of 2, thus increasing the brightness by a factor of 4.

V. Summary

Theoretical and experimental results are reported on the thermal lensing effect in optically pumped Nd:YAG rods. It was found that a YAG crystal exhibits a positive lens effect under pump radiation. Due to the birefringence in the crystal two focal points are obtained for each input power level depending on the polarization of the beam.

The thermal focusing effect of the rod is mainly caused by the temperature dependent variation of the refractive index. Focusing effects caused by a

Fig. 5. Experimental setup for the measurement of the end face curvature of a Nd:YAG crystal.

distortion of the flatness of the crystal ends are negligible.

The author acknowledges the technical assistance of D. Rice and C. F. Zahnow.

Appendix

From Eqs. (16) and (17) given in Koechner and Rice,[13] one obtains for the change of the indicatrix for a plane perpendicular to the [111] direction:

$$\Delta B_{x^*x^*} = \tfrac{1}{6}[p_{11}(3\epsilon_r + \epsilon_\Phi + 2\epsilon_x) + p_{12}(3\epsilon_r + 5\epsilon_\Phi + 4\epsilon_z)$$
$$+ 2p_{44}(3\epsilon_r - \epsilon_\Phi - 2\epsilon_z)], \quad (A1)$$

$$\Delta B_{y^*y^*} = \tfrac{1}{6}[p_{11}(\epsilon_r + 3\epsilon_\Phi + 2\epsilon_z) + p_{12}(5\epsilon_r + 3\epsilon_\Phi + 4\epsilon_z)$$
$$- 2p_{44}(\epsilon_r - 3\epsilon_\Phi + 2\epsilon_z)], \quad (A2)$$

where p_{11}, p_{12} and p_{44} are the elastooptical coefficients in a cubic crystal and ϵ_r, ϵ_Φ and ϵ_z are the radial, tangential, and axial strains in the rod, respectively.

The strains in a cylindrical rod can be expressed as follows[11, 14]

$$\epsilon_r = S'[(3\nu - 1) - (7\nu - 1)r^2/r_0^2], \quad (A3)$$

$$\epsilon_\Phi = S'[(3\nu - 1) - (5\nu - 3)r^2/r_0^2], \quad (A4)$$

and

$$\epsilon_z = S'[2(\nu - 1) - 4(\nu - 1)r^2/r_0^2]. \quad (A5)$$

where

$$S' = \alpha A_0 r_0^2/(1 - \nu)16K, \quad (A6)$$

α is the thermal expansion coefficient, ν is the Poisson ratio, and K is the thermal conductivity.

Introducing Eqs. (A3) to (A5) into (A1) and (A2) gives

$$\Delta B_{x^*x^*} = S(c'_x = c''_x r^2/r_0^2)/6, \quad (A7)$$

$$\Delta B_{y^*y^*} = S(c'_y - c''_y r^2/r_0^2)/6, \quad (A8)$$

where

$$S = \alpha \eta P_{in}/(1 - \nu)16K\pi L, \quad (A9)$$

and

$$c'_x = c'_y = 4(3\nu - 1)(p_{11} + 2p_{12} + p_{44})$$
$$+ 4(\nu - 1)(p_{11} + 2p_{12} - 2p_{44}), \quad (A10)$$

$$c''_x = 3(7\nu - 1)(p_{11} + p_{12} + 2p_{44})$$
$$+ (5\nu - 3)(p_{11} + 5p_{12} - 2p_{44})$$
$$+ 8(\nu - 1)(p_{11} + 2p_{12} - 2p_{44}), \quad (A11)$$

$$c''_y = (7\nu - 1)(p_{11} + 5p_{12} - 2p_{44})$$
$$+ 3(5\nu - 3)(p_{11} + p_{12} + 2p_{44})$$
$$+ 8(\nu - 1)(p_{11} + 2p_{12} - 2p_{44}). \quad (A12)$$

Equation (A9) is obtained from Eq. (A6) by substituting A_0 according to Eqs. (2) and (3).

With Eq. (13) the change in refractive index is

$$\Delta n_x^* = c_2 + c_3 r^2/r_0^2, \quad (A13)$$

and

$$\Delta n_y^* = c_4 + c_5 r^2/r_0^2, \quad (A14)$$

where

$$c_2 = c_4 = -n_0^3 S c'_x/12, \quad (A15)$$

$$c_3 = n_0^3 S c''_x/12, \quad (A16)$$

$$c_5 = n_0^3 S c''_y/12. \quad (A17)$$

References

1. L. M. Osterink and J. D. Foster, Appl. Phys. Lett. **12**, 128 (1968).

2. H. S. Carslow, *Conduction of Heat in Solids* (Clarendon Press, Oxford, England, 1952), p. 204.

3. M. Born and E. Wolf, *Principles of Optics* (Pergamon Press, London, 1965).

4. J. F. Nye, *Physical Properties of Crystals* (Oxford University Press, London, 1964).

5. H. Kogelnik, Bell. Syst. Tech. J. **44**, 455 (1965).

6. E. Snitzer and C. G. Young, in *Lasers*, A. K. Levine, Ed. (M. Dekker, New York, 1968), Vol. 2.

7. D. A. La Marre, "High Performance Laser Research," Report AD840913 American Optical Corp., June 1968.

8. R. W. Dixon, J. Appl. Phys. **38**, 5149, 1967.

9. "YAG:Nd Data," Union Carbide Corporation, Electronics Div., Crystal Products Dept.

10. J. D. Foster and L. M. Osterink, Appl. Opt. **7**, 2428 (1968).

11. W. Koechner, Appl. Opt. **9**, 1427 (1970).

12. H. Kogelnik, Proc. IEEE **54**, 1312 (1966).

13. W. Koechner and D. K. Rice, IEEE J. Quantum Electron. **QE-6**, 557 (1970).

14. S. Timoshenko and J. N. Goodier, *Theory of Elasticity* (McGraw-Hill, New York, 1951).

15. A. G. Fox and T. Li, Bell Syst. Tech. J. **40**, 453 (1961).